PHYSICAL REVIEW B VOLUME 61, NUMBER 10 1 MARCH 2000-II

Cutoff length in the logarithmic interaction between a vortex-antivortex pair in quench-condensed superconducting Bi films

M. M. Rosario, Yu. Zadorozhny, and Y. Liu
Department of Physics, The Pennsylvania State University, University Park, Pennsylvania 16802

(Received 26 April 1999; revised manuscript received 11 October 1999)

The current-voltage (I-V) characteristic of disordered superconducting Bi films prepared *in situ* in a ^{3}He cryostat by quench deposition has been studied. At a fixed temperature, a crossover from linear (Ohmic) to nonlinear (power-law) behavior was observed as the bias current was increased. An analysis of the data based on the theory of dynamic scaling was attempted. A unique value for the critical exponent is shown to be difficult to determine from the scaling alone. On the other hand, the features seen in the I-V curves can be accounted for using a simple picture of current-induced unbinding of vortex-antivortex pairs that involves a crossover from a logarithmic to an $1/r$ interaction between the vortex-antivortex pair. The implications of such an interaction for the nature of the two-dimensional superconductor-insulator transition are discussed.

I. INTRODUCTION

The nature of the superconducting transition in disordered two-dimensional (2D) superconductors has been a focus of attention in superconductivity research for the past few decades. Originally argued *not* to occur in 2D superconducting systems, the Kosterlitz-Thouless-Berezinskii (KTB) transition[1–3] was suggested by Beasley, Mooij, and Orlando[4] to be the correct description of the superconducting transition in high-resistance superconducting films. It was argued that in these films, the transverse penetration depth $\lambda_\perp = \lambda^2/d$ (where λ is the bulk penetration depth and d the film thickness) would become comparable to the system size in the transition regime. This allows for the logarithmic interaction between vortices to extend to lengths comparable with the sample. In this case, the vortex-antivortex pairs, which are bound at low temperatures, unbind at a well-defined transition temperature. In the decades following the original KTB work, the observation of a KTB transition has been reported in a variety of 2D superconducting systems.[5–11] Recently, however, this paradigm has come under question.

The revived interest stems primarily from the behavior of the current-voltage (I-V) characteristic. Within the framework of the standard KTB theory, the vortex-antivortex pair unbinding starts at the transition temperature T_c, where a discontinuous jump in the I-V exponent such that $V \sim I$ for $T > T_c$ and $V \sim I^3$ at $T = T_c$ is expected.[12] For temperatures below T_c, in the $I=0$ limit, $V \sim I^{\alpha(T)}$, with $\alpha(T) > 3$, and increasing as temperature is lowered. Recent studies in Josephson junction arrays[13–15] and cuprate superconductors[16,17] show a significant Ohmic deviation from the predicted power-law behavior at low temperatures *in the low current limit* and no universal jump in the exponent of the I-V curve that is expected from the KTB transition. In fact, a scrutiny of the published data on the KTB transition suggests that the low current Ohmic behavior, as well as the lack of a discontinuous jump, has been quite commonly observed previously.[6,9–11]

To reconcile these apparent discrepancies between the experimental results and the expectations of the KTB theory, a different approach based on the dynamic scaling theory of Fisher, Fisher, and Huse[18] has been proposed.[17,19] In this theory, the 2D normal-superconducting transition is assumed to be continuous, governed by a characteristic correlation length ξ and characteristic time τ, which diverge at the critical point with $\tau \sim \xi^z$, where z is the dynamic critical exponent. In the critical regime, all physical quantities, including I-V isotherms, should scale. Using the scaling form of Fisher, Fisher, and Huse, the I-V curves should collapse onto a scaling curve following

$$V = I\xi^{-z}\chi_{\pm}(I\xi/T), \tag{1}$$

where $\chi_{\pm}(x)$ is the scaling function for temperatures above/below T_c. Within the dynamic scaling picture, the standard KTB transition is characterized by a diffusive exponent $z=2$. A dynamic scaling analysis has been applied to various 2D systems and an apparently universal critical exponent $z \approx 5.6$ has been found. An exponent as large as 5.6 would suggest that the vortex-antivortex pair unbinding in these systems is highly collaborative in nature.

Alternatively, a finite-size scaling for the KTB transition has been developed to analyze the superconducting transition in various 2D systems.[13,14,16] Assuming an underlying KTB transition, this approach takes into account the presence of thermally excited free vortices due to the finite system size or finite cutoff length in the logarithmic interaction. Within this analysis, the interaction beyond $\lambda_\perp$ is simplified as a constant, rather than $1/r$ as shown originally by Pearl.[20] While the effect of the $1/r$ interaction is ignored, this approach appears capable of accounting for the main features seen in the I-V characteristic of 2D superconductors.

In this paper, we report our experimental studies of the superconducting transition in quench-condensed Bi films. We have used dynamic scaling to analyze our data. Although we are able to collapse the data onto a scaling curve, a unique value for the critical exponent cannot be obtained. On the other hand, we found that by taking into account the effect of a finite cutoff length in the logarithmic interaction between a vortex-antivortex pair, we can explain our experimental results quite well. Different from the finite-size scaling, this analysis does not require the occurence of a KTB transition in the 2D superconducting system. We have explicitly examined the effect of the $1/r$ dependence in the interaction between a vortex-antivortex pair for separation distances larger than $\lambda_{\perp}$. The crossover between logarithmic and $1/r$ interaction is shown to give rise to an Ohmic tail in the nonlinear I-V curves. Implications for the nature of the 2D superconductor-insulator (S-I) transition[21] will also be discussed.

II. EXPERIMENTAL SETUP

Ultrathin films of Bi were prepared *in situ* in a ^{3}He cryostat with a base temperature of 0.3 K. The homemade quench deposition system is installed in the inner vacuum can (IVC) of the ^{3}He cryostat. A small thermal evaporator is attached to the bottom tapered vacuum seal of the IVC, directly opposite the substrate. The evaporator is composed of four ceramic-metal electrical feedthroughs supplying current to two independent evaporation sources. All electrical elements are supported by a ceramic base for electrical insulation. The two homemade tungsten evaporation baskets are prewetted by the evaporation materials in a conventional room-temperature evaporator prior to cooling down. The residual strain in the tungsten wire is removed in this process to avoid uncontrolled deformations during the low-temperature depositions. A stainless sheet shields the two baskets from one another, which is necessary when evaporating two different materials. For the present study, both baskets were filled with Bi of 99.9999% purity. The evaporator is illustrated in Fig. 1(a).

Films were deposited atop a glazed alumina substrate mounted on a copper sample stage, which, in turn, is in thermal contact with the ^{3}He pot. The sample stage is shielded from the evaporation sources and the inner wall of the IVC by a copper cylinder with a shutter, both thermally anchored to the 1 K pot. A rail and gear system, connected to a linear motion feedthrough on top of the cryostat, opens and closes the shutter. Since the vacuum can is immersed in a liquid-helium bath, the cryopumping of the IVC walls provides an ultrahigh vacuum environment. Bismuth was evaporated at a constant rate of 0.1 to 1 Å/s, as monitored by two 6-MHz quartz crystal thickness monitors mounted on the copper cylinder, adjacent to the substrate as shown in Fig. 1(b). The uncovered sensor monitors the evaporation rate at all times to help ensure that the shutter will be opened only after a stable evaporation rate is established. The other sensor remains shielded until the deposition begins. Film geometry is defined by a copper shadow mask mounted 0.5 mm above the substrate. During the Bi deposition the substrate temperature remains below 8 K, as monitored by a thermometer mounted adjacent to the substrate. After deposition, the film is kept below 15 K to prevent annealing.

Electrical leads made of 100-Å-thick Au film evaporated at room temperature allow four-wire electrical transport measurements. Measurements were made as a function of current and temperature. The current from a Keithley 220 dc current source was reversed for each point to eliminate voltages due to thermal offset.

While the morphology of these quench condensed Bi films have not been studied directly, reentrant superconductivity has been observed in thinner films which are superconducting locally, but not globally. Therefore we believe that these quench condensed Bi films are actually granular, although each grain itself should be amorphous.

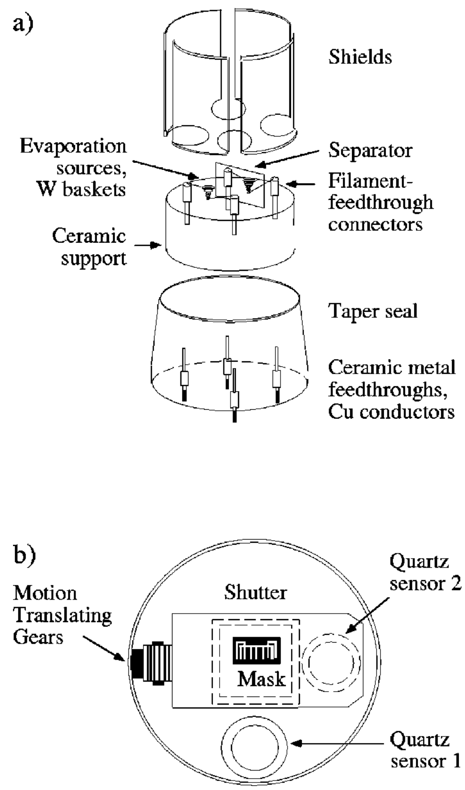

FIG. 1. (a) Thermal evaporator mounted in the taper seal at the bottom of the IVC. The distance between the substrate and evaporation source is approximately 12 cm. During deposition of Bi, the substrate temperature remains below 8 K. (b) Two quartz sensors for monitoring and measuring the deposition rate and film thickness. A copper shadow mask defining the film geometry is shown.

III. RESULTS

In Fig. 2, values of normalized resistance are plotted against temperature for two films prepared in separate runs. The thinner film, film 1, has a superconducting transition regime wider than film 2, as expected since the thinner film is more disordered. The high-temperature part of the resistive transitions can be described by the Aslamasov-Larkin theory for paraconductivity effects.[22] Fitting the data to the expression for conductance results in a mean-field transition temperature $T_{co}=3.90\pm0.02$ K for film 1, and 5.790 ± 0.005 K for film 2. Alternatively, one can determine values of T_{co} based on $R_{\square}(T_{co})=R_{\square}^{n}/2$, where $R_{\square}^{n}$ is the normal-state sheet resistance, which yields $T_{co}=3.94$, 5.780 K for films 1 and 2, respectively. The values of T_{co} determined by fitting to the conductance expression and by finding the midpoint resistance are seen to agree with one another.

The I-V characteristic at various temperatures in the superconducting transition regime for film 1 is shown in Fig. 3. The curves exhibit a crossover between two distinct power-law behaviors, $V\sim I^{\alpha_{1,2}(T)}$ where $\alpha_1(T)$ and $\alpha_2(T)$ are exponents in the low and high current regimes. Fitting the above

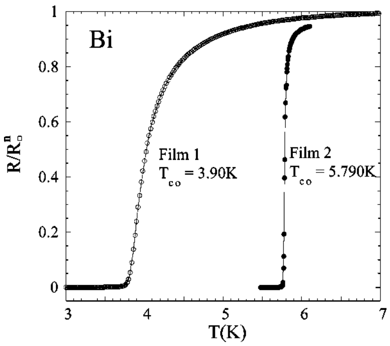

FIG. 2. Normalized resistances plotted against temperature for films 1 and 2. The measuring current was 1 μA. The superconducting transition temperatures, determined by a fit to the Aslamasov-Larkin theory are indicated. Film 1 is nominally 25 Å thick with $R^{n}_{\square}=1.74$ kΩ. Film 2, with $R^{n}_{\square}=91$ Ω, has a nominal thickness of 50 Å.

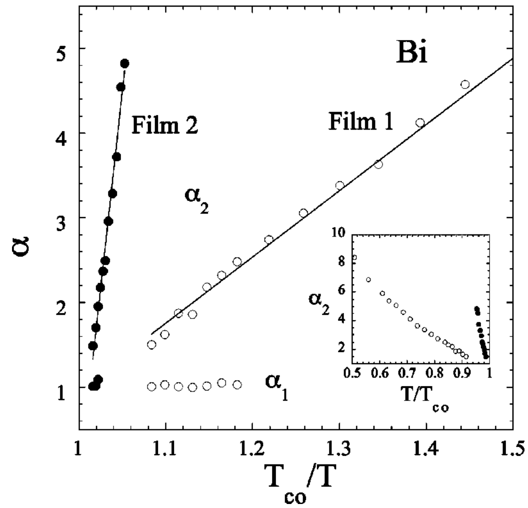

FIG. 4. Exponents determined by fitting the data to a power law in the low (α_1) and high (α_2) bias current regimes for films 1 and 2, represented by open and filled circles, respectively. The lines are fits to $1/T$ dependence. The inset shows the lack of a discontinous jump in α_2 in the transition regime.

form to the data in the respective current regimes yields values of $\alpha_1(T)$ and $\alpha_2(T)$ which are plotted in Fig. 4 for films 1 and 2. For all temperatures, the exponent for the high bias current part of the I-V characteristic is larger than 1 and increases as $1/T$ as temperature is lowered. In comparison, the low current tails seen in the I-V curves are essentially linear at relatively high temperatures and slightly superlinear at lower temperatures. The crossover may be further described by a crossover current, $I_{\rm cross}$. As illustrated in Fig. 3, $I_{\rm cross}$ is experimentally defined by extrapolating the power-law behaviors in the low and high current regimes at a fixed temperature. Values of $I_{\rm cross}$ are shown in Fig. 5 to have a linear dependence on temperature. At the lowest temperatures, the crossover appears to fall below the noise floor of our measurements. Although the data are not shown, similar behavior has been observed in other films prepared in a separate run.

Within the standard picture of KTB transition, the logarithmic interaction between a vortex-antivortex pair extends over the entire sample, such that $\lambda_{\perp} \gg W$, where W is the sample size. Above $T_{\rm c}$, the system is populated by thermally induced free vortices, as well as a number of already bound pairs. In the presence of a small applied current these free vortices produce Ohmic behavior, i.e., $V \sim I$. The vortex correlation length $\xi_{+}(T)$, which may be thought of as the size of the largest bound vortex pair, is nonzero but significanty smaller than W. As temperature decreases, $\xi_{+}(T)$ grows and more vortices and antivortices are bound in pairs. At $T_{\rm c}$, $\xi_{+}(T)$ diverges resulting in all vortices being bound and a zero resistance state is reached. This zero resistance state only holds in the zero current limit.[11] For $T \leqslant T_{\rm c}$, applying a current leads to the unbinding of pairs. The weakly interacting pairs with large separations will be broken by a small applied current, while the strongly bound, closely separated vortices can only be unbound by a large applied current. The current-induced unbinding of pairs leads to a power law behavior of $V \sim I^{\alpha(T)}$ where $\alpha(T) \geqslant 3$. Traditionally, $T_{\rm c}$ is defined by $\alpha(T_{\rm c})=3$. Thus the signature of the transition, as seen in the I-V characteristic, is a discontinuity in the I-V behavior from Ohmic to power law as temperature is

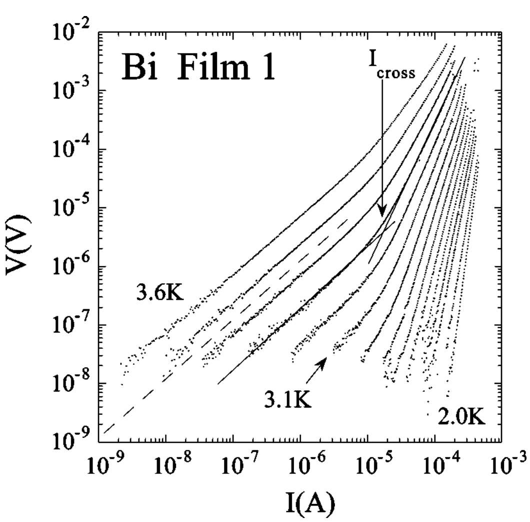

FIG. 3. Current-voltage characteristics of film 1. From top to bottom, the temperatures are 3.6, 3.5, 3.4, 3.3, 3.2, 3.1, 3.0, 2.9, 2.8, 2.7, 2.6, 2.5, 2.4, 2.2, and 2.0 K. The $T=3.1$ K curve exhibits $V \sim I^3$ dependence in the high current regime. The dashed line represents linear behavior. A crossover current $I_{\rm cross}$, is defined as indicated.

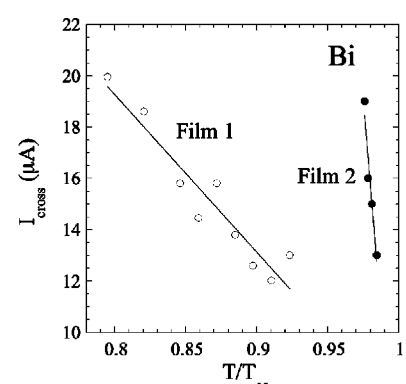

FIG. 5. Values of the crossover current $I_{\rm cross}(T)$ plotted against $T/T_{\rm co}$ for films 1 and 2. Linear fits are indicated by straight lines.

lowered past T_c. In addition, the resistance at $T > T_c$ is governed by flux flow and may be described by the Halperin-Nelson resistance formula[12] $R \sim \exp[-2\sqrt{b(T_{co}-T)/(T-T_c)}]$ where b is a nonuniversal constant.

We have attempted to fit this resistance formula to our data in the lower part of the superconducting transition region. If we choose as the critical curve the one corresponding to $\alpha_2 = 3$, then $T_c = 3.1$ K. The Halperin-Nelson formula fits the data over a small temperature range near T_c of roughly two orders of magnitude in the film resistance. However, a discontinuous jump in the exponent is not observed at any temperature, by tracking either the low or high current limit. The high-current exponent $\alpha_2(T)$ varies continuously with, perhaps, a kink at $\alpha_2 = 3$ as seen in the inset of Fig. 4. The disappearance of an Ohmic tail at $T = 2.8$ K corresponds to an exponent of 4.6. These observations seem to suggest that a true KTB transition did not occur in these quench condensed Bi films.

IV. DYNAMIC SCALING

Assuming that the normal-superconductor transition in 2D is a continuous phase transition, the physics in the critical region is dominated by τ and ξ which diverge as $\xi \sim |T - T_c|^{-v}$ and $\tau \sim \xi^z$ as T_c is approached, where v and z are the correlation length and the dynamic scaling exponent, respectively. The scaling theory[17–19] suggests that the I-V characteristic follows

$$I^{z+1}/[VT^z] = \varepsilon_{\pm}(I^z\xi^z/T^z), \tag{2}$$

where $\varepsilon_{\pm}(x) \equiv x/\chi_{\pm}(x^{1/z})$ and $\chi_{\pm}(x)$ is the scaling function above/below T_c, and ξ is assumed to be symmetric about T_c with the standard KTB form. Note that this form is identical to Eq. (1). At T_c, the above equation reduces to $V \sim I^{z+1}$. Above T_c, $R(T) \sim \xi^{-z}$ so that $x = I^z/R(T)T^z$. Varying z effectively redefines the transition's universal jump from $1 \rightarrow 3$ to $1 \rightarrow z+1$, wherein $z+1$ corresponds to the exponent of the first fully nonlinear I-V curve. In addition, the Halperin-Nelson resistance formula is modified to $R \propto \exp[-z\sqrt{b(T_{co}-T)/(T-T_c)}]$. The standard KT features are recovered when $z = 2$. A scaling analysis of various systems, including superconducting films, Josephson junction arrays, and superfluid ^{4}He films, has recently been carried out,[19] and has yielded an apparently system-independent critical exponent $z \approx 5.6$. Such a large z has been speculated to follow from the vortex-antivortex pairs unbinding by exchanging members with neighboring pairs. In particular, a steady state recombination process involving four vortices would result in $z = 6$.

The value for z and T_c were obtained from the highest temperature I-V curve that follows power law, $V \sim I^{z+1}$, over all currents. By inspecting the I-V curves shown in Fig. 3, we have $z = 3.6$ and $T_c = 2.70$ K. A scaling collapse of the I-V characteristic shown in Fig. 3 following the procedure described above is displayed in Fig. 6, with $z = 3.6$. Ideally, the value of T_c can be obtained independently from fitting the resistive transition to the modified Halperin-Nelson formula. The results so obtained could be used as a self-consistent check. However, the value of z cannot be independently determined from this fitting. Given this, and the fact that the scaling ansatz is not explicitly dependent upon T_c, this fit is not attempted. Within the dynamic scaling theory, the values of resistance used in the scaling collapse should be determined in the Ohmic regime. At low temperatures, an Ohmic regime cannot be defined in our data. As a result, we have treated the resistance as a fitting parameter in our analysis, with the values shown in Table I. As a comparison, the resistance values obtained directly from the I-V curves for which an Ohmic regime can be identified are also listed. It can be seen that these values are similar to those obtained from the fitting. While departure from the scaling curve at low currents is visible in several I-V isotherms in the low current limit, the collapsing of curves appears to work, which suggests that the superconducting-normal transition in this film may indeed be a continuous phase transition. The unusually large critical regime, from 3.5 to 2.7 K, may be explained by assuming a large correlation length. On the other hand, the question of the usefulness of this approach remains. As shown in Fig. 7(a), we have attempted to scale the data using $z = 5.6$ (and $T_c \approx 2.45$ K from Fig. 3), with the

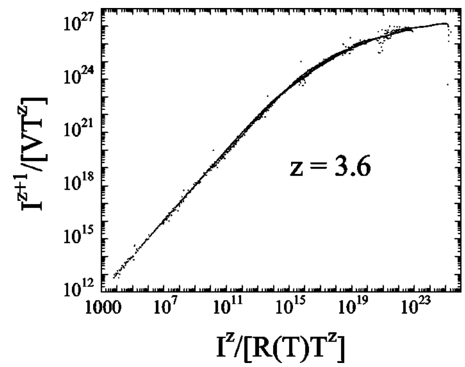

FIG. 6. Scaling of the I-V characteristic from Fig. 3, with $z = 3.6$ (and $T_c = 2.7$ K). Both axes are in arbitrary units. Only the lower branch corresponding to $T > T_c$ is shown. The resistances used as fitting parameters are listed in Table I.

TABLE I. Resistance values used in the scaling analyses of the IV characteristic of Fig. 3. The values for Ohmic resistances are given where applicable. R_1 and R_2 are the resistances used in the $z = 3.6$ and $z = 5.6$ *and* 6.86 scaling analyses, respectively. Only resistances used for scaling in the lower branch are listed.

T(K)	$R_{\mathrm{Ohmic}}(\Omega)$	$R_1(\Omega)$	$R_2(\Omega)$
3.5	2.0	2.0	2.0
3.4	0.7	0.7	0.7
3.3	0.2	0.174	0.2
3.2	0.047	0.031	0.047
3.1	0.012	0.006	0.014
3.0	0.004	0.0004	0.003
2.9		1.4×10^{-5}	3.3×10^{-4}
2.8		1.0×10^{-7}	5.0×10^{-5}
2.7			5.0×10^{-6}
2.6			3.0×10^{-7}
2.5			1.0×10^{-8}
2.4			2.0×10^{-10}
2.2			1.0×10^{-12}

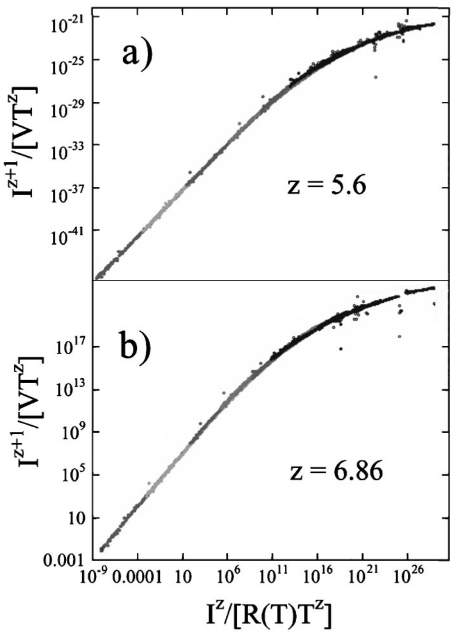

FIG. 7. Scaling analyses corresponding to (a) $z=5.6$ and (b) $z=6.86$. Both axes are in arbitrary units. Only the lower branch of the transition is shown. The resistances used in the analyses are listed in Table I.

resistance again being a fitting parameter. It is interesting to note that, as shown in Fig. 7(b), the data can also be collapsed onto a scaling curve with $z=6.86$ (and $T_c=2.2$ K from Fig. 3), using the *exact* same resistance values used for the $z=5.6$ scaling, suggesting that a collapse of the data alone cannot yield a unique value for z. While this uncertainty in determining the critical exponent may not necessarily amount to a serious challenge to the fundamental validity of dynamic scaling theory, the above analysis suggests that one must be cautious in drawing conclusions based on the value of z obtained from the scaling analysis.

V. VORTEX-ANTIVORTEX UNBINDING WITH A FINITE $\lambda_\perp$

Taking into account finite-size effects,[13,14,16] the conventional KTB theory has been modified to treat the experimental observations in various 2D superconducting systems. In this picture, several length scales are present in the problem. These lengths include the vortex correlation length $\xi_+(T)$, the cutoff length in the logarithmic interaction $\lambda_\perp$, the current length r_c, and the finite size of the sample W. An underlying KTB transition is assumed to occur at $T=T_c$. Above and below $T=T_c$, the finite size $\mathcal{L}(=\min[\lambda_\perp,W])$ leads to a nonzero density of thermally induced free vortices, different from the conventional KTB transition. An applied current probes the dynamics of vortex-antivortex pairs with separations *larger* than the current length r_c. Therefore sufficiently small currents probe the behavior of vortex-antivortex pairs with separations *larger* than $\mathcal{L}$, essentially the free vortices/antivortices, resulting in Ohmic behavior.

Above T_c, the competing lengths are r_c and $\xi_+(T)$. The use of a finite current leads to current-induced free vortices/antivortices which gives rise to a nonlinear I-V characteristic when $r_c \approx \xi_+(T)$. However, a finite $\mathcal{L}$ introduces certain complications. Ohmic behavior is expected when $r_c \gg \min[\mathcal{L},\xi_+(T)]$. In this picture, since $\xi_+(T) \ll \mathcal{L}$ for temperatures well above T_c, a crossover from Ohmic to nonlinear behavior occurs at a current $I_{\rm cross}$ which is dependent on $\xi_+(T)$. At temperatures near T_c, $\xi_+(T)$ diverges and the crossover is governed by $\mathcal{L}$. Therefore $I_{\rm cross}$ is strongly temperature dependent for $T>T_c$ but weakly temperature dependent for $T \gtrsim T_c$. The Ohmic behavior for $T<T_c$ is solely dependent on $r_c \gg \mathcal{L}$, with the crossover occurring at $r_c \approx \mathcal{L}$. If the vortex-antivortex interaction beyond $\lambda_\perp$ is constant instead of $1/r$, the crossover should occur at $I_{\rm cross} \sim 4k_bT_cWe/\pi\hbar\mathcal{L}$.[19] The above-described theory qualitatively accounts for the low current Ohmic behavior seen in a number of systems, in particular in Josephson-junction arrays of finite size.[13,14] However, an objection has been raised in Ref. 17 that a transition from KTB to non-KTB behavior cannot be tuned by varying the array size, as alluded to in previous studies,[14,16] citing that W and $\lambda_\perp$ affect the density of free vortices in the same manner. In addition, this approach assumes the occurence of a KTB transition, despite a finite sized $\lambda_\perp$. It should be noted that it is upon such a finite transverse penetration depth that Kosterlitz and Thouless based their argument against the occurence of a phase transition in 2D superconducting systems.[1]

We propose that the features observed in the I-V characteristics in the present study may be explained by a simple treatment which does not require the existence of a KTB transition. Within this model, the behavior is determined by the current-induced vortex-antivortex pair unbinding, wherein the members of the bound pair interact either logarithmically or as $1/r$ and are unbound by a current driven through the system. For completeness, we begin with the nondisordered, unrenormalized pair potential $\phi(r)$ given by[20]

$$2E_{c_1} - d\left(\frac{\phi_o}{4\pi\lambda}\right)^2 \ln\left(\frac{\lambda}{r}\right) \quad \text{for} \quad \xi<r<\lambda_\perp, \tag{3a}$$

$$2E_{c_2} - \frac{(\phi_o/2\pi)^2}{r} \quad \text{for} \quad r>\lambda_\perp, \tag{3b}$$

where E_{c_1} and E_{c_2} are constants associated with the energy of the vortex normal core, d the film thickness, $\phi_o=hc/2e$ the flux quantum, and ξ the superconducting coherence length which is the effective radius of the vortex normal core. In the presence of an applied current, the potential energy of a pair changes to $U(\mathbf{r},\theta)=\phi(r)-(J_s\phi_o/c)r\cos\theta$, where θ is the angle between $\mathbf{J}_s$ and $\mathbf{r}$. The potential is smallest at $\theta=0$. In this direction, a saddle point is found at r_c, the current length, with its value depending on J_s. Classical escape over this saddle point leads to pair unbinding and free vortices/antivortices.

The electrical resistance of the film is proportional to the vortex mobility,[23] which, in turn, is proportional to the density of free vortices, n_f. In a steady state of a two-body recombination process, $n_f \sim \Gamma^{1/2}$ where Γ is the rate of ionization controlled by a Boltzmann factor, $\Gamma \sim e^{-U(\mathbf{r}_c,0)/k_bT}$. Given this, the I-V characteristic can be obtained using $V \sim In_f \sim I\Gamma^{1/2}$. As $\phi(r)$ has different forms for $r<\lambda_\perp$ and for $r>\lambda_\perp$, so does the I-V behavior for small and large currents. At small currents, $r_c=(hc/8\pi^2 eJ_s)^{1/2}>\lambda_\perp$, leading to $\Gamma \sim e^{2(I/I_o)^{1/2}}$, where $I_o=(\pi k_B T)^2 cA/\phi_o^3$ (A is the cross-sectional area). At large currents, $r_c=\hbar n_s e/2mJ<\lambda_\perp$. This leads immediately to $\Gamma \sim e^{(\pi n_s \hbar^2/2mk_B T)\ln I}$ (where $n_s=n_s^{2D}=n_s^{3D}d$). Therefore we have

$$V \sim I^{1+\pi n_s \hbar^2/4mk_B T} \quad \text{for} \quad \xi<r<\lambda_\perp \tag{4a}$$

$$V \sim I e^{(I/I_o)^{1/2}} \quad \text{for} \quad r>\lambda_\perp . \tag{4b}$$

Examining the data shown in Fig. 4, we can see that the I-V characteristic agrees with this finite cutoff length picture. In the high bias current region, the resistance is dominated by vortex-antivortex pairs with small separations. For these pairs, the interaction is logarithmic resulting in $V \sim I^{\alpha_2(T)}$, with $\alpha_2(T)=1+\pi n_s \hbar^2/4mk_B T$. Furthermore, using the mean-field result of $n_s=n_s(T)=n_s(0)(1-T/T_{\rm co})$ results in $\alpha_2(T) \sim 1/T$. The $1/T$ dependence of α_2 is clearly seen for both films. Values of $n_s(0)$ may be determined from the slopes shown in Fig. 4, and are found to be $4.4\times 10^{12}/\mathrm{cm}^2$ and $7.8\times 10^{13}/\mathrm{cm}^2$ for films 1 and 2, respectively.

As the bias current is lowered, the cutoff length becomes important, resulting in a crossover of the I-V characteristic to $V \sim I e^{(I/I_o)^{1/2}}$. In this regime, an estimate of I_o yields a value at least an order of magnitude larger than the applied current. Given that $I_o \gg I$, a linear IV characteristic is expected, as observed experimentally. As temperature is lowered, values of I_o decrease and the exponential factor may begin to affect the I-V behavior at small currents. This effect is qualitatively seen in the low-temperature curves as a deviation from purely Ohmic behavior.

The validity of such a simple treatment is further tested by examining the temperature dependence of the crossover current $I_{\rm cross}$. The crossover corresponds to $r_c \sim n_s/I_{\rm cross}$. Using the mean-field result for n_s and assuming that $\lambda_\perp$ is temperature independent in this small temperature range, $I_{\rm cross}$ should be linearly dependent on temperature. This linear dependence was observed experimentally as shown in Fig. 5.

If many pairs are present in the film, which is expected below $T=T_{\rm co}$, the pair potential for a vortex-antivortex pair of a given separation will be modified by the presence of other pairs with smaller separation (screening effects), leading to a renormalized pair potential. In addition, the disorder present in the film will introduce pinning forces, further modifying the pair potential. A full analysis of renormalization effects is obviously complicated. Given that our experimental results seem to agree with the expectations of the unrenormalized theory, it seems that the renormalization effect does not change the picture qualitatively. However, quantitative changes are expected, for example, the cutoff length may be modified due to the screening effects.

VI. IMPLICATIONS ON THE S-I TRANSITION

The present work suggests that a cutoff length in the logarithmic interaction between a vortex-antivortex pair is significantly smaller than the sample size in quench condensed Bi films, and that the effects of the logarithmic and $1/r$ forms of the vortex interaction are observable. This has potential consequences on the nature of the zero-temperature ($T=0$) superconductor-insulator (S-I) transition,[21] which has been shown to occur in quench-condensed Bi films.[24]

This quantum phase transition can be traversed by tuning disorder, carrier concentration, applied magnetic field, or film thickness.[21] A dirty boson Hubbard model[25–27] has been put forward to describe this phenomenon. Within this model, the superconducting state is characterized by a condensate of Cooper pairs and localized vortices, while in the insulating phase Cooper pairs are localized and vortices are mobile. The model predicts that if the system is self-dual, namely, if the model describing the system is invariant when expressed in terms of charge or vortex degree of freedom, a universal resistance at $T=0$ given by $h/4e^2$ will emerge at the S-I transition. So far, the values of the critical resistance observed experimentally in various systems seem to vary substantially,[21,28] which raises the question concerning the validity of the theory. An additional parameter[29] or a metallic phase[30] has to be included in the theory to account for the apparent disagreement between the dirty boson Hubbard theory and experiment.

Is it possible that a real experimental system can be made self-dual? Within the dirty boson model, there are at least two difficulties for films of metals to be considered self-dual for the S-I transition in zero magnetic field.[27] First, the particle-hole symmetry possessed by vortex-antivortex pairs does not exist for Cooper pairs. Mukhopadhay and Weichman[31] have examined the issue concerning the lack of particle-hole symmetry at the S-I transition theoretically and concluded that although such a symmetry is not present in the original Hamiltonian, a statistical version is restored at the critical point. Second, the interaction between charged pairs and that between vortices, are, in general, dissimilar. The Coulomb interaction between Cooper pairs has a $1/r$ form, while the interaction between a vortex-antivortex pair is logarithmic, up to $\lambda_\perp$. It has been shown that in materials of high dielectric constant, the interaction between two charges may be described as logarithmic up to a cutoff length, beyond which it recovers the $1/r$ form.[32] The presence of a cutoff length in the logarithmic interaction between charges has been experimentally observed in various 2D systems.[33–36]

The form of interaction between charges as described above is identical to that between vortices in this system, as shown in the present work. If the effective dielectric constant for insulating Bi films is large, as may be expected,[37] the interaction between Cooper pairs may also be logarithmic with a finite cutoff length. In this case, the system will be self-dual at least in principle. However, since the interaction between charges and that between vortices may be modified by the disorder and many-body effects differently, whether a particular sequence of films can actually have the same interaction form for Cooper pairs and vortices may depend strongly on the film preparation, and substrate conditions. Consequently, a self-dual system may not always be achieved even in the same material system prepared under nominally the same conditions. The characterization of the behavior of a self-dual system must await for these experimental issues to be resolved.

VII. SUMMARY

We have carried out electrical transport measurements in disordered superconducting Bi films prepared *in situ* in a

^{3}He cryostat by quench deposition. A crossover from linear (Ohmic) to nonlinear behavior was observed in the I-V characteristics in the superconducting transition regime. We have analyzed the data by the dynamic scaling theory and, alternatively, by examining the current-induced vortex-antivortex unbinding involving a cutoff length in the logarithmic interaction between vortex-antivortex pairs. The dynamic scaling does not seem yield a unique value for the critical exponent z. However, the latter approach explains our results well.

It is known that the presence of a $T=0$ S-I transition will affect the behavior of the system at finite temperatures. In the critical region of this quantum phase transition, the system should scale because of the presence of a quantum critical point at $T=0$. It will be interesting to push the current study to the regime close to the S-I transition. In particular, if the current approach shows that the interaction between the vortex-antivortex pairs on the superconducting side and that between charges on the insulating side of the S-I transition in the same sequence of films have the same form, the system will be self-dual. Interesting phenomena may be found if such a system can be prepared.

ACKNOWLEDGMENTS

We acknowledge useful discussions with Dr. S. Pierson, Dr. M. Friesen, and Dr. A. Hebard. This work was supported by the National Science Foundation through Grant No. DMR-9702661.

[1] J.M. Kosterlitz, J. Phys. C **7**, 1046 (1974).
[2] J.M. Kosterlitz and D.J. Thouless, J. Phys. C **6**, 1181 (1973).
[3] V.L. Berezinskii, Zh. Éksp. Teor. Fiz. **59**, 907 (1970) [Sov. Phys. JETP **32**, 493 (1971)].
[4] M.R. Beasley, J.E. Mooij, and T.P. Orlando, Phys. Rev. Lett. **42**, 1165 (1979).
[5] D.J. Resnick, J.C. Garland, J.T. Boyd, S. Shoemaker, and R.S. Newrock, Phys. Rev. Lett. **47**, 1542 (1981).
[6] A.F. Hebard and A.T. Fiory, Phys. Rev. Lett. **50**, 1603 (1983).
[7] D.W. Abraham, C.J. Lobb, M. Tinkham, and T.M. Klapwijk, Phys. Rev. B **26**, 5268 (1982).
[8] A.F. Hebard and A.T. Fiory, Phys. Rev. Lett. **44**, 291 (1980).
[9] P.A. Bancel and K.E. Gray, Phys. Rev. Lett. **46**, 148 (1981).
[10] K. Epstein, A.M. Goldman, and A.M. Kadin, Phys. Rev. Lett. **47**, 534 (1981).
[11] A.M. Kadin, K. Epstein, and A.M. Goldman, Phys. Rev. B **27**, 6691 (1983).
[12] B.I. Halperin and D.R. Nelson, J. Low Temp. Phys. **36**, 599 (1979).
[13] M.V. Simkin and J.M. Kosterlitz, Phys. Rev. B **55**, 11 646 (1997).
[14] S.T. Hebert, Y. Jun, R.S. Newrock, C.J. Lobb, K. Ravindran, H.-K. Shin, D.B. Mast, and S. Elhamri, Phys. Rev. B **57**, 1154 (1998).
[15] H.S.J. van der Zant, H.A. Rinken, and J.E. Mooij, J. Low Temp. Phys. **79**, 289 (1990).
[16] J.M. Repaci, C. Kwon, Qi Li, X. Jiang, T. Venkatessan, R.E. Glover, C.J. Lobb, and R.S. Newrock, Phys. Rev. B **54**, R9674 (1996).
[17] S.M. Ammirata, M. Friesen, S.W. Pierson, L.A. Gorham, J.C. Hunnicutt, M.L. Trawick, and C.D. Keener, Physica C **313**, 225 (1999).
[18] D.S. Fisher, M.P.A. Fisher, and D.A. Huse, Phys. Rev. B **43**, 130 (1991).
[19] S.W. Pierson, M. Friesen, S.M. Ammirata, J.C. Hunnicut, and L.A. Gorham, Phys. Rev. B **60**, 1309 (1999).
[20] J. Pearl, in *Low Temperature Physics-LT9*, edited by J.G. Daunt, D.O. Edwards, F.J. Milford, and M. Yaqub (Plenum, New York, 1965), p. 566.
[21] See, for example, N. Markovic and A.M. Goldman, Phys. Today **51** (11), 39 (1998); N. Markovic, C. Christiansen, A.M. Mack, W.H. Huber, and A.M. Goldman, Phys. Rev. B **60**, 4320 (1999); and references cited therein.
[22] L.G. Aslamasov and A.I. Larkin, Fiz. Tverd. Tela (Leningrad) **10**, 1104 (1968) [Sov. Phys. Solid State **10**, 875 (1968)].
[23] M. Tinkham, *Introduction to Superconductivity* (McGraw Hill, New York, 1996), Chap. 8.
[24] Y. Liu, K.A. McGreer, B. Nease, D. Haviland, G. Martinez, J.W. Halley, and A.M. Goldman, Phys. Rev. Lett. **67**, 2068 (1991).
[25] M.P.A. Fisher, Phys. Rev. Lett. **65**, 923 (1990).
[26] M.P.A. Fisher, P.B. Weichman, G. Greinstein, and D.S. Fisher, Phys. Rev. B **40**, 546 (1989).
[27] M.-C. Cha, M.P.A. Fisher, S.M. Girvin, M. Wallin, and A.P. Young, Phys. Rev. B **44**, 6883 (1991).
[28] Y. Liu, D.B. Haviland, B. Nease, and A.M. Goldman, Phys. Rev. B **47**, 5931 (1993).
[29] N. Mason and A. Kapitulnik, Phys. Rev. Lett. **82**, 5341 (1999).
[30] D. Das and S. Doniach, Phys. Rev. B **60**, 1261 (1999).
[31] R. Mukhopadhay and P.B. Weichman, Phys. Rev. Lett. **76**, 2977 (1996).
[32] L.V. Keldysh, Zh. Éksp. Teor. Fiz. **29**, 716 (1979) [JETP Lett. **29**, 658 (1979)].
[33] J.E. Mooij, B.J. van Wees, L.J. Geerligs, M. Peters, R. Fazio, and G. Schön, Phys. Rev. Lett. **65**, 645 (1990).
[34] R. Yamada, S. Katsumoto, F. Komori, and S. Kobayashi, J. Phys. Soc. Jpn. **62**, 2229 (1993).
[35] T.S. Tighe, M.T. Tuominen, J.M. Hergenrother, and M. Tinkham, Phys. Rev. B **47**, 1145 (1993).
[36] Y. Liu and J.C. Price, Mod. Phys. Lett. B **9**, 939 (1994).
[37] W. Jones and N.H. March, *Theoretical Solid State Physics* (Dover Publication, New York, 1973), Vol. 2, p. 852.